ACS SENSORS

Article

Cite This: ACS Sens. 2019, 4, 1072−1080

pubs.acs.org/acssensors

Development of a Minimally Invasive Microneedle-Based Sensor for Continuous Monitoring of β-Lactam Antibiotic Concentrations in Vivo

Sally A. N. Gowers,*[,†] David M. E. Freeman,[†] Timothy M. Rawson,[‡] Michelle L. Rogers,[†] Richard C. Wilson,[‡] Alison H. Holmes,[‡] Anthony E. Cass,[§] and Danny O'Hare[†]

[†]Department of Bioengineering, Imperial College London, London SW7 2AZ, United Kingdom

[‡]National Institute for Health Research Health Protection Research Unit in Healthcare Associated Infections and Antimicrobial Resistance, Imperial College London, London W12 0NN, United Kingdom

[§]Department of Chemistry & Institute of Biomedical Engineering, Imperial College London, London SW7 2AZ, United Kingdom

Supporting Information

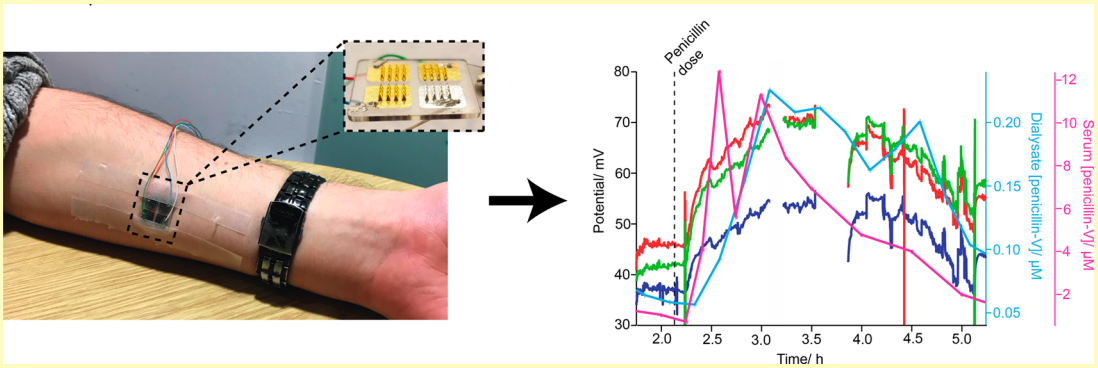

ABSTRACT: Antimicrobial resistance poses a global threat to patient health. Improving the use and effectiveness of antimicrobials is critical in addressing this issue. This includes optimizing the dose of antibiotic delivered to each individual. New sensing approaches that track antimicrobial concentration for each patient in real time could allow individualized drug dosing. This work presents a potentiometric microneedle-based biosensor to detect levels of β-lactam antibiotics in vivo in a healthy human volunteer. The biosensor is coated with a pH-sensitive iridium oxide layer, which detects changes in local pH as a result of β-lactam hydrolysis by β-lactamase immobilized on the electrode surface. Development and optimization of the biosensor coatings are presented, giving a limit of detection of 6.8 μM in 10 mM PBS solution. Biosensors were found to be stable for up to 2 weeks at −20 °C and to withstand sterilization. Sensitivity was retained after application for 6 h in vivo. Proof-of-concept results are presented showing that penicillin concentrations measured using the microneedle-based biosensor track those measured using both discrete blood and microdialysis sampling in vivo. These preliminary results show the potential of this microneedle-based biosensor to provide a minimally invasive means to measure real-time β-lactam concentrations in vivo, representing an important first step toward a closed-loop therapeutic drug monitoring system.

KEYWORDS: *β-lactam antibiotic monitoring, minimally invasive, continuous monitoring, antibiotic resistance, microneedle array, electrochemical biosensors, iridium oxide, in vivo monitoring*

Antimicrobial resistance (AMR) represents a major global health challenge. Recent reports on the impact of AMR have predicted that by 2050 a continued rise in drug-resistant infections could lead to up to 10 million deaths every year.[1] AMR is caused by a combination of factors, but major drivers are known to be inappropriate/misuse of antibiotics.[2] As a result, there is a critical need to select the optimal antimicrobial dose and dosing regimen in order to maximize therapeutic efficacy while minimizing any harmful consequences such as resistance or toxicity.[3]

Current treatment practices have led to a wide variability in therapeutic antibiotic concentrations across patients due to differences in individual pharmacokinetic parameters.[4] These findings have contributed to a growing consensus that antimicrobial therapy should be personalized in order to account for this variability and therefore to optimize dosage accuracy and hence patient care.[5]

Current therapeutic drug monitoring (TDM) approaches rely on discrete blood measurements. Such sampling methods are invasive and limit the temporal resolution of the

Received: February 8, 2019
Accepted: April 5, 2019
Published: April 5, 2019

DOI: 10.1021/acssensors.9b00288
ACS Sens. 2019, 4, 1072−1080

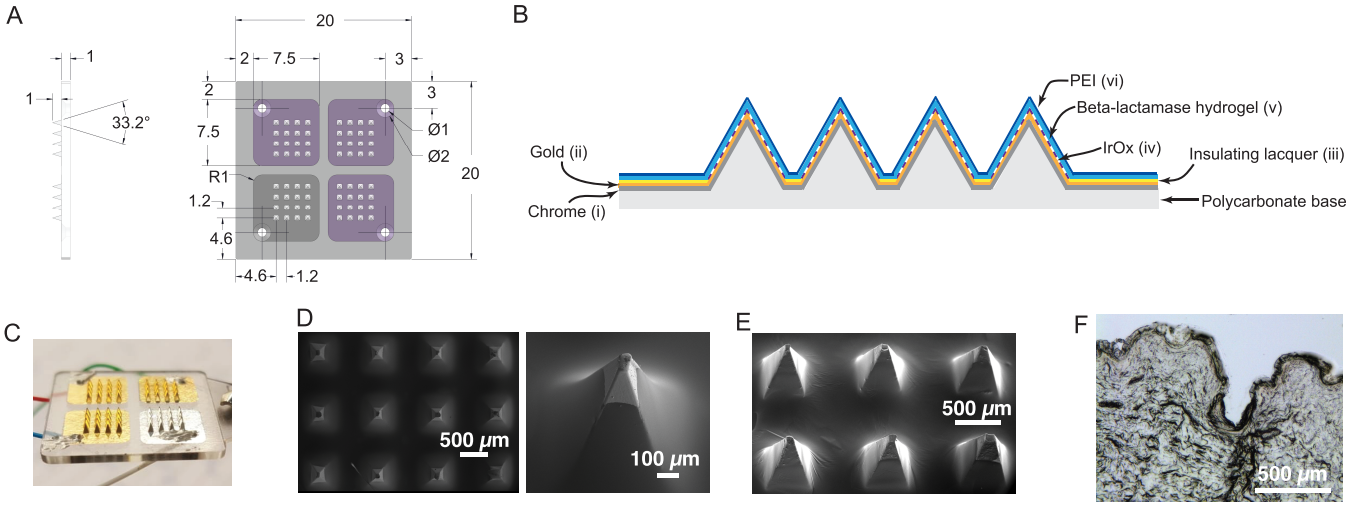

Figure 1. (A) Schematic of microneedle array showing dimensions in mm (thanks to Torr Scientific for the array drawing). (B) Schematic cross-section of working electrode microneedles showing each layer. The poly(carbonate) base is first sputter-coated with chrome (i) and then coated with gold by e-beam evaporation (ii). The base of the arrays is coated with an insulating lacquer (iii) so that only the spikes are conducting. Iridium oxide (iv) is deposited onto the gold electrode by applying a fixed potential of +0.6 V vs a Ag|AgCl reference electrode. A β-lactamase containing hydrogel is deposited on top of the iridium oxide layer (v) and once cured a layer of PEI (vi) is deposited on top of the hydrogel for mechanical stability. (C) Photo of microneedle array consisting of four metallized sets of microneedles, three coated with gold and one (bottom right-hand side in photo) with silver. (D) Scanning electron microscopy (SEM) image of gold microneedle array. Bases are insulated with lacquer so that only tips are exposed. (E) SEM image of microneedle array coated with iridium oxide and enzyme hydrogel layers (thanks to Dr. Hyejeong Song and Dr. Marsilea Booth for SEM images). (F) Photo showing 20 μm cross-section of human skin after microneedle application (thanks to Sharad Patel and Dr. Claire Higgins for assistance in skin application experiments).

information obtained. Moreover, they are labor intensive and not practical in a clinical environment. There is an urgent need for a minimally invasive approach for TDM that can provide real-time measurements of antimicrobial concentrations and allow individualized patient dosing.

Various biosensing technologies have been developed for detection of antimicrobials across a wide range of applications.[6−10] In particular, considerable research efforts have been devoted to measurement of levels of β-lactam antibiotics,[11−27] a class of commonly used broad-spectrum antibiotic to which penicillin derivatives belong, due to the high incidence of bacteria developing resistance to this class of antimicrobial drug. However, translation of these sensing strategies for real-time drug monitoring has been limited to invasive techniques such as microdialysis or devices that extract interstitial fluid.[8,28,29] Such devices are not practical outside of controlled environments, such as critical care, due to their invasive nature and the intensity of sampling required. A minimally invasive method of tracking antibiotic concentration is required to enable TDM for all situations involving administration of β-lactam antibiotics.

There is rapidly growing interest in the use of transdermal microneedle-based electrodes for molecular-based sensing[30−34] and drug delivery.[35−38] Examples of microneedle-based biosensors have been shown for continuous monitoring of metabolic markers such as glucose and lactate[30,31] as well as for the drug theophylline[31] and for organophosphate nerve agents.[32] These sensors only penetrate the *stratum corneum* layer of skin and therefore do not cause pain or draw blood as they do not reach the nerve endings and capillary blood vessels in the dermis. As a result, such sensors provide a minimally invasive means of sampling the interstitial fluid for drug or metabolite monitoring.

In this paper, we present the development of a minimally invasive microneedle-based biosensor for continuous detection of β-lactam antibiotic levels in real time. The microneedle arrays have shown demonstrable efficacy in human trials for measurement of glucose.[30] The needle dimensions ensure a reasonable fraction penetrate the viable epidermis and no deeper. The biosensor employs an iridium oxide pH-sensing layer to detect local changes in pH arising from hydrolysis of β-lactam antibiotics by β-lactamase. A similar approach was first reported in 1974, using a glass pH electrode coated with penicillinase to detect penicillin.[39] Iridium oxide offers an alternative to a glass pH electrode and was chosen due to its improved stability, fast response time and low impedance.[40] Optimization of the biosensor is shown along with proof-of-concept in vivo data from a healthy volunteer to demonstrate the potential of this technology.

EXPERIMENTAL SECTION

Materials and Reagents. β-Lactamase (extended spectrum) from ex-microbial source was obtained from Sekisui Enzymes. All other reagents were obtained from Sigma-Aldrich. Electrical wires and insulating varnish were obtained from RS Components.

Microneedle Construction. Poly(carbonate) microneedle arrays were fabricated by Professor Nikolaj Gadegaard at the University of Glasgow using injection molding. The poly(carbonate) arrays were metallized at Torr Scientific (Bexhill, UK). Four separate areas of microneedles were first sputter-coated with an initial seed layer of chrome (110 nm). Following this, three sections (forming the working electrodes) were coated with 150 nm of gold by e-beam evaporation and the final section (forming the reference electrode) was coated with 150 nm of silver by e-beam evaporation (Figure 1A, C).

The metallized arrays were wired to gold contacts using silver epoxy (Circuitworks, Chemtronics). Insulating varnish (RS Components) was applied on top of the cured silver epoxy and allowed to wick in between the individual microneedles in order to insulate the base of the microneedle array while leaving the tips of the microneedles exposed (Figure 1D). For each electrode, around 10 μL of insulating varnish was added via syringe with a wide bore needle

DOI: 10.1021/acssensors.9b00288
ACS Sens. 2019, 4, 1072−1080

(18G). Each electrode was tested by cyclic voltammetry in a solution of ferrocene monocarboxylic acid to ensure that the silver epoxy had been completely insulated.

Sensor Fabrication. The biosensors are fabricated in several layers as shown in Figure 1B. Before functionalization, the insulated microneedle arrays were cleaned with 70% ethanol in deionized water and dried with a stream of compressed air. The first layer involved electrodeposition of iridium oxide onto the gold working electrodes to create a pH sensitive layer. To do this, an iridium oxalate solution was prepared following the method described by Yamanaka et al.[41] Briefly, 1 mL of hydrogen peroxide (30% w/w) was added to a 4.5 mM solution of iridium(IV) chloride hydrate in deionized water with light stirring. The solution was stirred for 10 min and 0.5 g of oxalic acid dihydrate was added. Again, the solution was stirred for 10 min and anhydrous potassium carbonate was added until pH 10.5 was reached. The solution was left to stabilize at room temperature for 2 days, in which time the solution turned violet in color.

Iridium oxide was electrodeposited onto the microneedle tips from the iridium oxalate solution by applying +0.6 V (vs a Ag|AgCl reference electrode) to the working electrode for 300 s. A platinum mesh was used as the counter electrode. After this initial electrodeposition step, the electrode was left in the solution for 10 min and the process was repeated two further times. The array was then washed with deionized water and dried with a stream of compressed air.

To create the Ag|AgCl reference electrode, the silver pad of the array was chloridized with sodium hypochlorite (10−15% available chlorine) solution (10 μL) for 30 s. The electrode was washed thoroughly with deionized water and dried with a stream of compressed air. A control hydrogel mixture was made containing 1.25% (v/v) poly(ethylenimine) (PEI, branched, average M_w = 25 000 Da), 5% (v/v) glycerol and 3.705 mg/mL poly(ethylene glycol) diglycidyl ether (PEG-DE, average M_n 500 Da) in 10 mM phosphate buffered saline (PBS). The control hydrogel mixture (10 μL) was applied to both the reference electrode and any gold electrodes to be used as a control or ground for in vivo studies. The array was clamped with the needles facing down to encourage the hydrogel to cover the tips and was cured at 45°C for 2 h. For the working electrodes, an enzyme hydrogel was made containing 125 mg/mL β-lactamase, 1.25% (v/v) PEI, 5% (v/v) glycerol and 18.5 mg/mL PEG-DE in 10 mM PBS. This hydrogel mixture (10 μL) was carefully applied to each gold electrode to be used as a sensor. This mixture represents the optimized sensor hydrogel composition. The optimization protocol to arrive at this recipe is described in the results section below. The array was clamped with the needles facing down to encourage the hydrogel to cover the tips of the microneedles. The hydrogel was cured at 45°C for 2 h.

A final layer of 5% (v/v) PEI in 10 mM PBS (5 μL) was applied to each electrode to provide mechanical stability and the arrays were left upside down at room temperature for 1 h to dry (Figure 1E). Arrays were stored in the freezer at −20°C until use.

Sensor Sterilization. Sensor arrays were sent to TCM Associates Ltd. (Essex, UK) for gamma irradiation with 25 kGy of cobalt-60 irradiation in accordance with ISO 11137-2 standards.

Sensor Calibration. To carry out pH calibrations, the array was immersed in 10 mM PBS solutions of varying pH (adjusted by addition of hydrochloric acid or sodium hydroxide) in the range of pH 4.5−8.0 (determined using a Mettler Toledo SevenEasy pH meter and Hanna Instruments pH probe). The array was left in each solution for approximately 5 min until the potential stabilized. The open circuit potential was recorded versus a Ag|AgCl reference electrode using in-house electronics.

To carry out penicillin calibrations, the array was immersed in a stirred solution of 10 mM PBS and allowed to equilibrate for 30 min. Aliquots of 0.5 M penicillin G sodium salt or 0.5 M penicillin V potassium salt solution in 10 mM PBS were added in increasing amounts so as to change the cumulative concentration of penicillin in the beaker. After each addition, the sensor was allowed to stabilize for 5 min. The open circuit potential was recorded compared to a Ag|AgCl reference electrode using in-house electronics.

For studies investigating the long-term stability of the sensors, penicillin calibrations were carried out repeatedly over a two-week period. The sensor array was stored in the freezer at −20 °C in between calibrations.

Reference Electrode Stability Studies. To test the stability of the Ag|AgCl reference electrode potential on the array, the reference electrode was placed in a beaker of 10 mM PBS (pH 7.4) and the open circuit potential was measured versus a commercial Ag|AgCl reference electrode (BASi, US) over several hours.

Skin Application Studies. To visualize microneedle application, microneedles were applied to a biopsy of human skin. These studies were carried out with the help of Sharad Patel and Dr. Claire Higgins. After application, the microneedles were removed, the sample was frozen, and 20 μm cross-sections were taken using a cryostat. Images of these cross-sections were taken using a light microscope, as shown in Figure 1F. This photo shows an indentation that is 460 μm deep and 410 μm wide. The indentation depth and width will vary depending on how far through the spike indentation the cross-section is taken. Indentations were seen at a separation of 1.9 mm, which is consistent with the indentations being caused by spike application; based on the array dimensions, spikes could be seen at 1.5−2.12 mm apart, depending on the orientation of the sample.

In Vivo Study. In vivo trials were carried out with healthy volunteers. All procedures were approved by the London-Harrow Research Ethics Committee (reference 18/LO/0054). In each case, two separate arrays, a control array and a sensing array, were placed on the inner forearm and were secured with tape. The sensing array comprised three working electrodes functionalized with the enzyme hydrogel and a Ag|AgCl reference electrode. The control array comprised three working electrodes functionalized with the control hydrogel and a Ag|AgCl reference electrode.

The open circuit potential of the three sensing working electrodes and one control working electrode were measured continuously in real time vs a Ag|AgCl reference electrode using in-house electronics. The remaining two working electrodes of the control array were connected to ground. The Ag|AgCl reference electrode of the control array was not connected in this case. Open circuit potentials were measured for approximately 6 h during which time the participant was free to move in their chair. The arrays were temporarily disconnected from the electronics if greater movement was required. The participant began the study after 5 doses of penicillin V potassium (500 mg taken every 4−6 h by mouth) and took a final dose approximately midway through the monitoring period at an appropriate time based on their most recent dose. Both sensing and control arrays were calibrated in vitro following removal after application.

If participants consented, a microdialysis probe was also inserted subcutaneously in the forearm by a qualified clinician. The skin was cleaned and an anesthetic cream (EMLA cream 5%) was applied 45 min prior to probe insertion followed by topical application of ice. A sterile CMA63 microdialysis probe (MDialysis, 10 mm membrane length, 20 kDa molecular-weight cutoff) was inserted subcutaneously using a tunnelling needle and introducer and secured in place using Tegaderm transparent dressings. The probe was perfused with sterile T1 perfusion solution (MDialysis) at 2 μL/min using a CMA107 microdialysis pump (MDialysis). Samples of dialysate were collected into microvials every 15 min. At the end of the study the vials were frozen at −80°C and sent to a laboratory for HPLC analysis.

Blood sampling was performed at predetermined intervals to provide data for the pharmacokinetic profile of penicillin V in blood. Time points were selected based on the known population pharmacokinetics of penicillin V.[42,43] Samples were collected via a cannula with the first 3 mL of blood taken discarded. Samples were allowed to clot for 15 min and then kept on ice until they were spun down and frozen at a −80°C. All samples were frozen within 45 min of being collected.

DOI: 10.1021/acssensors.9b00288
ACS Sens. 2019, 4, 1072−1080

RESULTS AND DISCUSSION

Sensor Characterization. The pH response of an iridium oxide-coated microneedle array was tested in PBS solutions of different pH values between 4.5 and 8 (Figure 2A purple line).

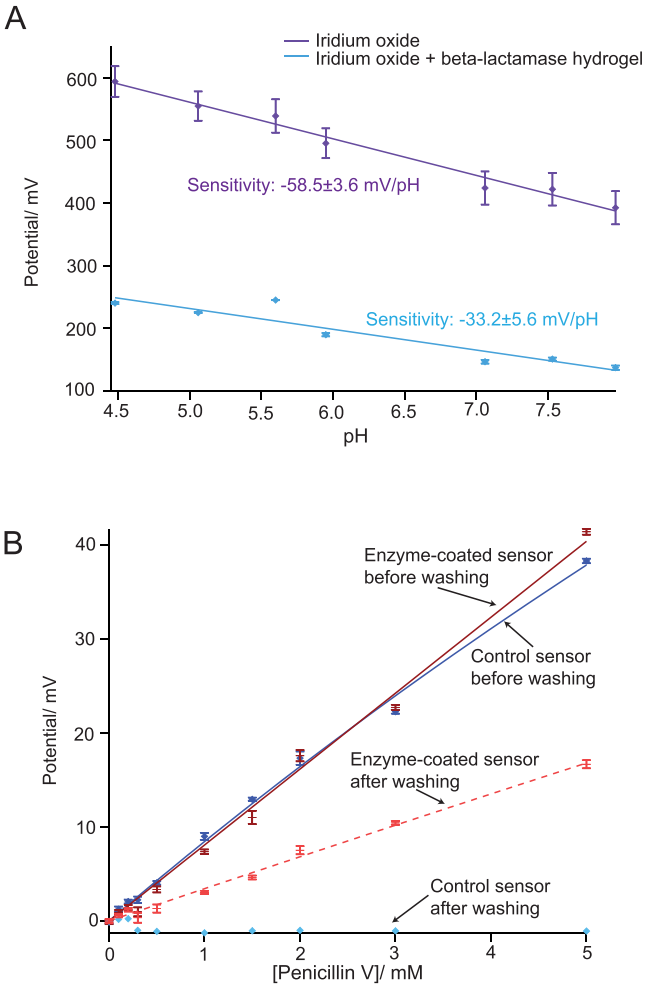

Figure 2. (A) pH response of microneedles coated with iridium oxide layer only (purple) and iridium oxide and β-lactamase hydrogel layers (blue). Potential is measured vs a AgIAgCl reference electrode. Markers represent mean ± standard deviation of measurement. (B) Response of enzyme-coated (25 mg/mL β-lactamase, 1% (v/v) glycerol, 3.7 mg/mL PEG-DE in 10 mM PBS) and control sensors to increasing concentrations of penicillin V in a stirred beaker of 10 mM PBS before washing and after washing in a stirred beaker of 10 mM PBS for 5.5 h. Potentials are measured vs a AgIAgCl reference electrode and the background potential has been subtracted from the measurements. Markers represent mean ± standard deviation.

As shown in Figure 2A, in this pH range, there is a linear relationship between the open circuit potential of the iridium oxide-coated electrodes and pH value. The slope of this line is Nernstian, as expected.

The effect of functionalizing the iridium oxide-coated electrode with an enzyme-containing hydrogel layer was investigated by testing the pH response of the sensor after addition of the hydrogel layer (Figure 2A blue line). As shown in Figure 2A, the addition of this hydrogel layer leads to an offset in the y-axis and a decrease in the sensitivity of the sensor to changes in pH. We hypothesize that the offset seen here is caused by chloride ions in the solution leading to removal of some of the iridium oxide layer over repeated calibrations and is not in fact due to the hydrogel layer; we have found that addition of the hydrogel layer actually protects the sensor against this to some extent. The decrease in sensitivity seen upon addition of the hydrogel layer is likely due to the buffer capacity of this layer arising from basic functional groups the PEI and enzyme in the gel.

For initial investigations, the hydrogel consisted of PEG-DE cross-linked to β-lactamase only. To verify the response of the fully functionalized biosensor to penicillin, an enzyme-coated sensor and a control sensor were both immersed in a beaker of PBS in which step changes in penicillin concentration were created. As shown in Figure 2B (solid lines), both the enzyme-coated and control sensors responded equally to increasing concentrations of penicillin. Previous studies, however, had shown that without the enzyme-coated sensor in the same beaker, the control sensor did not respond to penicillin (data not shown). Therefore, the response seen when the enzyme-coated and control sensors are placed in the same beaker could be either caused by cross-talk between the sensors or could be due to enzyme being washed out into the solution and reacting with penicillin in solution. To test these possible explanations, the enzyme-coated and control sensors were calibrated again after a washing step where the sensors were left in a stirred solution of PBS for 5.5 h in between calibrations. As shown in Figure 2B (red dotted line and light blue markers), after this washing step, a loss in sensitivity was seen for the enzyme-coated sensor and the control sensor no longer responded to penicillin. This indicates that in the initial calibration before the washing step, enzyme was diffusing out of the hydrogel into the solution causing the control sensor to also respond to penicillin. The next step was to attempt to optimize the hydrogel composition to try and reduce this effect and therefore improve sensor stability.

Sensor Optimization. The sensors tested in Figure 2B did not have any additional cross-linker in the hydrogel; the enzyme was immobilized by cross-linking of PEG-DE with amine groups on the enzyme.[44] As shown in Figure 2B, this led to enzyme leaking out into the solution. To try to better encapsulate the enzyme in the hydrogel, the PEG-DE content was varied (Figure 3A). As shown in Figure 3A, the difference seen in the sensor response with differing hydrogel PEG-DE concentration was small. Moreover, no decrease in cross-talk was seen as a result of changing the PEG-DE concentration (Supporting Information, Figure S1).

In order to improve the sensor response and solve the issue of cross-talk, an additional polymer, poly(ethylenimine) (PEI) was added to the hydrogel in varying concentrations (Figure 3B). As shown in Figure 3B, addition of PEI led to a slight decrease in the value of E_{max} (the maximum potential at which the enzyme is saturated by the substrate) compared with Figure 3A without PEI; increasing the PEI concentration in the hydrogel led to improved sensitivity, higher values of E_{max} and Km_{app}, and improved dynamic range; however, it also led to a slower response time (T_{90}) due to hindered diffusion through the hydrogel. Importantly, the addition of the PEI improved the issue of cross-talk, although did not remove it entirely (Supporting Information, Figure S2). As the changes we are interested in are not likely to be fast, the highest concentration (1.25% PEI) was chosen going forward in order to optimize the sensor response.

For in vivo studies, only the microneedle tips would be in contact with interstitial fluid. Therefore, the effect of insulating

DOI: 10.1021/acssensors.9b00288
ACS Sens. 2019, 4, 1072−1080

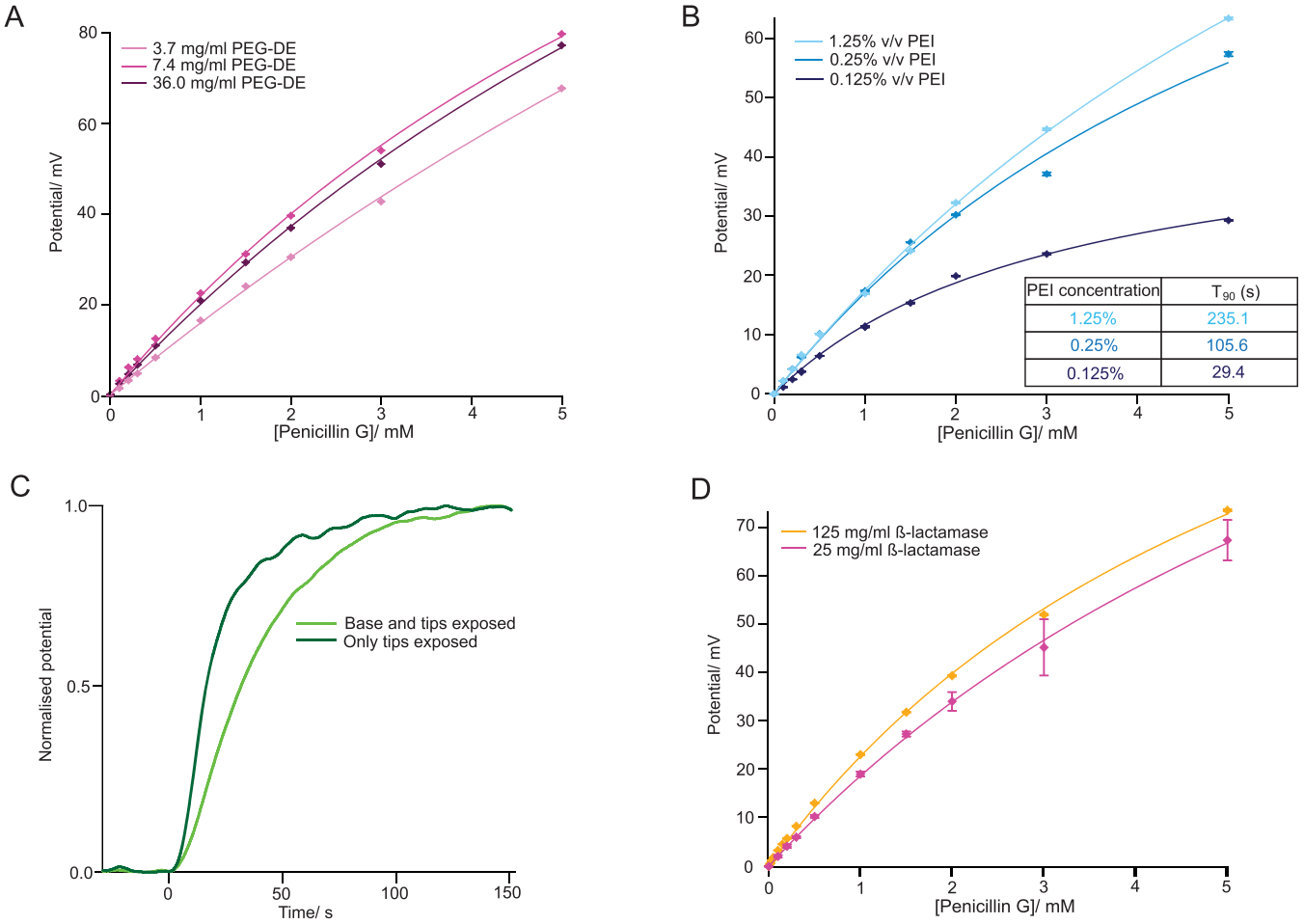

Figure 3. (A) Effect of enzyme-hydrogel PEG-DE concentration on calibration working curves for varying concentrations of penicillin G. PEG-DE concentrations tested were 3.7, 7.4, and 36.0 mg/mL (other hydrogel components: 25 mg/mL β-lactamase, 1% (v/v) glycerol in 10 mM PBS). Potential is plotted as change from baseline level. Markers represent mean ± standard deviation of measurement. Markers fit with Michaelis–Menten equation. (B) Effect of enzyme-hydrogel PEI concentration on calibration curves for varying concentrations of penicillin G. PEI concentrations investigated were 0.125%, 0.25% and 1.25% (v/v) (other hydrogel components: 25 mg/mL β-lactamase, 3.7 mg/mL PEG-DE, 1% (v/v) glycerol in 10 mM PBS). Markers represent mean minus background potential ± standard deviation of measurement. Markers fit with Michaelis–Menten equation. Inset table compares the T_{90} time response for each PEI concentration. (C) Effect of insulating base of microneedle pad on temporal response of sensors to a step change in penicillin G concentration. Responses have been normalized for comparison. Response when base is left exposed (light green) is compared to that when base is insulated and only tips are exposed (dark green). This investigation was done in parallel to the hydrogel optimization studies therefore hydrogel recipe was not yet optimized (hydrogel: 25 mg/mL β-lactamase, 3.7 mg/mL PEG-DE, 0.25% PEI, 1% (v/v) glycerol in 10 mM PBS). (D) Effect of enzyme concentration in hydrogel on calibration curves for varying concentrations of penicillin G. β-lactamase concentrations investigated were 25 and 125 mg/mL (hydrogels: 25 mg/mL β-lactamase, 3.7 mg/mL PEG-DE, 1.25% PEI, 1% (v/v) glycerol in 10 mM PBS and 125 mg/mL β-lactamase, 18.525 mg/mL PEG-DE, 1.25% PEI, 5% (v/v) glycerol in 10 mM PBS, respectively keeping the enzyme/PEG-DE/glycerol ratios constant). Only tips were exposed in both cases. Markers represent mean ± standard deviation (n = 3). Markers fit with Michaelis–Menten equation. All calibrations were carried out in a stirred beaker of 10 mM PBS. The potential was measured versus a AglAgCl reference electrode and the background potential was subtracted from the measurement.

the bases and having just the tips exposed was investigated (Figure 3C). A small reduction in sensitivity was seen with only the needle tips exposed, however, the sensor response time was faster. In addition, by insulating the base, the beaker calibration was more akin to the in vivo situation.

The final step in sensor optimization was to investigate the effect of varying the enzyme concentration (Figure 3D). As shown, in Figure 3D, a higher enzyme loading resulted in a slightly improved E_{max} and sensitivity and was therefore used for in vivo trials. For the higher enzyme loading case, the concentration of PEG-DE and glycerol was also increased to keep the relative ratio constant.

The final hydrogel composition consisted of 125 mg/mL β-lactamase, 18.5 mg/mL PEG-DE, 1.25% (v/v) PEI, and 5% (v/v) glycerol in 10 mM PBS, coated onto microneedles with only tips exposed. For in vivo trials, an outer layer of PEI was also cast on top of the hydrogel. This was initially tested in an effort to further reduce the cross-talk, however, no difference was observed. It has, however, been shown to provide mechanical stability.[40] The limit of detection for the optimized composition is 6.8 ± 1.04 μM (n = 3) in 10 mM PBS solution. In reality, although the buffer capacity of interstitial fluid is not known, it is likely to be considerably lower than that of 10 mM PBS (a conservative estimate chosen for testing). Dose–response curves in lower buffer capacity PBS solutions, which more closely represent the likely buffer capacity of interstitial fluid show improved limits of detection (Supporting Information, Figure S3).

DOI: 10.1021/acssensors.9b00288
ACS Sens. 2019, 4, 1072–1080

Stability Studies. To investigate the long-term stability of the fully functionalized biosensors, repeated penicillin calibrations were carried out over a two-week period. Representative data is shown in Figure 4A. The biosensors were stored in the freezer at −20°C in between calibrations. An initial drop in sensitivity was seen between calibrations carried out on days 1 and 3, however, this is consistent with the initial wash out of enzyme from the hydrogel layer seen in Figure 2B. After the initial drop in sensitivity, the sensor remained stable over the two-week period with a sensitivity in the linear region of 10.8 ± 0.35 mV/mM (mean ± standard deviation, n = 3). These results suggest that it is better to calibrate after application to avoid an initial wash out of enzyme from the hydrogel layer.

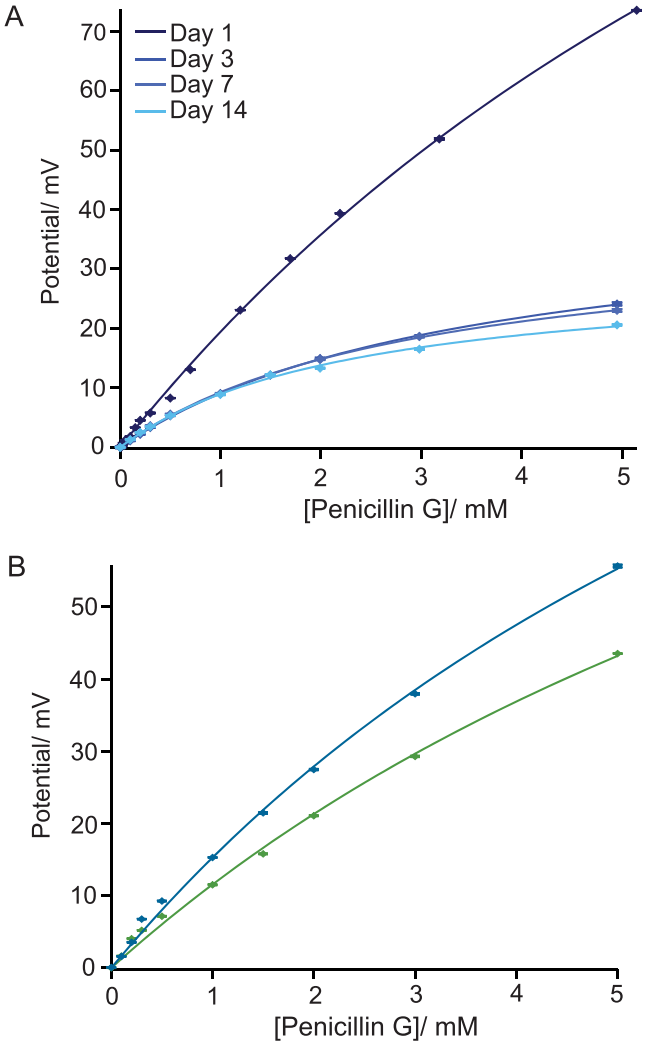

Figure 4. (A) Stability of biosensor calibration for varying concentrations of penicillin G over 2 weeks. Potential measured versus a AglAgCl reference electrode and is plotted as change from baseline level. Markers represent mean ± standard deviation of measurement. Markers fit with Michaelis−Menten equation. (B) Effect of sterilization on biosensor dose−response for varying concentrations of penicillin G. Response shown for two different biosensors. Potential measured vs a AglAgCl reference electrode and is plotted as change from baseline level. Markers represent mean ± standard deviation of measurement. Markers fit with Michaelis−Menten equation.

For their eventual use in critically ill patients, it is necessary to be able to sterilize the biosensors to prevent possible infection and improve patient safety. However, common methods of sterilization could lead to reduced sensitivity. Therefore, the sensor response was tested after gamma irradiation (TCM Associates, 25 kGy cobalt-60 irradiation). Figure 4B shows the response of two sterilized biosensors to increasing concentration of penicillin; the sensors still responded well after sterilization. Therefore, for patient studies, the sensors can be sterilized before use.

It was also important to verify the stability of the AglAgCl reference electrode on the array over the potential monitoring period. This was done by measuring the open circuit potential versus a commercial AglAgCl reference electrode in 10 mM PBS over a 10 h time period. After an initial 30 min stabilization period during which the potential drifted by 3.8 mV, the reference electrode potential was stable to within 0.5 mV for up to 6 h, which was adequate for in vivo studies. This reference electrode was coated with the control hydrogel, which increased stability.

In Vivo Studies. A proof-of-concept study was carried out to test the feasibility of using these microneedle biosensors for real-time monitoring of penicillin levels in vivo. Two arrays were positioned on the forearm of a healthy volunteer. Three β-lactamase-functionalized microneedle pads on one array and a control microneedle pad from the second array were monitored continuously in real time. Figure 5A shows the response of the three β-lactamase-functionalized microneedle pads over the monitoring period. The control response has been subtracted to account for drift. Measurements began after the participant had taken five doses of penicillin (500 mg every 4−6 h). A final dose was typically taken just over 2 h into the study (indicated by dotted line in Figure 5A). All three sensors show a similar trend, with open circuit potentials increasing after the final penicillin dose was taken, plateauing after an hour and then slowly decreasing. Although preliminary results appear to show that the sensors responded to changes in penicillin levels, it is not possible to quantify the magnitude of these changes using an in vitro beaker calibration as mass transport conditions will be different.

Levels of penicillin were also measured in the interstitial fluid every 15 min using microdialysis and in the blood by taking discrete blood samples every 15−30 min. These measurements are shown alongside the sensor results in Figure 5A. In these preliminary results, the sensor responses seem to track both dialysate and serum trends. Dialysate levels will be lower than the true tissue concentration due to probe recovery being less than 100%. However, even accounting for this, the levels measured are very low and close to the limit of detection of our biosensors in 10 mM PBS. We are currently carrying out further optimization of the sensor performance to ensure we can reliably measure changes occurring at such low levels in vivo.

In each case, biosensors were calibrated after removal following skin application to verify that the layers were intact. Representative data is shown in Figure 5B; the biosensors showed a good response to increasing concentrations of penicillin. This shows that the layers survived application with good activity. This was also confirmed by scanning electron microscopy (SEM) imaging, as shown in Figure 5C, showing minimum damage and intact layers after application.

CONCLUSION

We have developed and optimized a minimally invasive microneedle-based biosensor for continuous monitoring of β-

DOI: 10.1021/acssensors.9b00288
ACS Sens. 2019, 4, 1072−1080

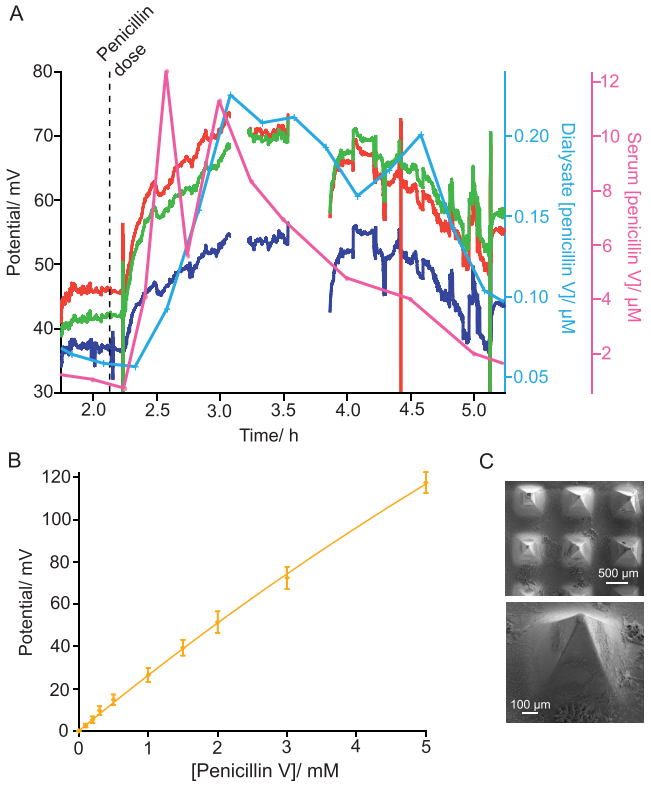

Figure 5. (A) In vivo response of three β-lactamase biosensors applied to a healthy volunteer (red, green, and dark blue traces). Gaps in data correspond to times when the sensors were temporarily disconnected so that the volunteer could move around. Control response has been subtracted from each trace to remove effects of drift that are common to both. Dialysate levels of penicillin V from a microdialysis probe inserted subcutaneously in the forearm are shown in light blue. Samples were taken every 15 min. Serum levels of penicillin V are shown in pink. Blood samples were taken every 15–30 min. All measurements have been time-aligned. Time 0 corresponds to the first blood sample collection. The dotted line indicates the point at which a final dose of penicillin was taken. (B) Post-use dose response curve for microneedle biosensor calibrated after application for 6 h in a healthy volunteer. Markers fitted to the Michaelis–Menten equation. Potential measured vs a Ag|AgCl reference electrode and is plotted as change from baseline level. Markers represent mean ± standard deviation of measurement. (C) SEM images of microneedles post-application showing functional layers still in place (thanks to Dr. Hyejeong Song and Dr. Marsilea Booth for SEM images).

lactam antibiotics in the interstitial fluid in real time. Although an initial wash-out of some of the immobilized enzyme was seen upon placing the biosensors in solution, they were found to be stable over a 2-week period and repeated measurements when stored at −20°C. Good sensitivity was seen after sterilization, an important requirement for fabrication of in vivo sensors. Following application of the microneedle-based sensors for 6 h, the functional layers were found to remain intact and dose response curves showed that sensitivity was maintained. We have demonstrated the capabilities of these biosensors for real-time tracking of penicillin concentrations in vivo in a proof-of-concept trial with healthy volunteers. Preliminary data indicate that levels track blood and microdialysis levels. However, with this particular drug, interstitial concentrations were found to be very low and at the limit of detection of our sensors. Current work is being carried out to further improve the limit of detection and to trial this sensing technology with other β-lactam antibiotics, where interstitial drug concentrations are likely to be higher. This real-time β-lactam sensor could be coupled to a closed-loop control system to provide real-time information on tissue drug concentrations for personalized drug dosing.

■ ASSOCIATED CONTENT

Supporting Information

The Supporting Information is available free of charge on the ACS Publications website at DOI: 10.1021/acssensors.9b00288.

Effect of PEG-DE and PEI hydrogel concentration on cross-talk; effect of calibration solution buffer capacity on sensor response (PDF)

■ AUTHOR INFORMATION

Corresponding Author

*E-mail: s.gowers11@imperial.ac.uk.

ORCID

Sally A. N. Gowers: 0000-0002-2407-2266

Anthony E. Cass: 0000-0001-8881-4786

Notes

The authors declare no competing financial interest.

■ ACKNOWLEDGMENTS

We would like to acknowledge Dr. Hyejeong Song and Dr. Marsilea Booth for assistance with SEM imaging, Sharad Patel and Dr. Claire Higgins for assistance with skin application experiments, and Professor Nikolaaj Gadegaard for manufacture of the poly(carbonate) microneedle arrays. We would also like to thank Dr. Sanjiv Sharma for his helpful advice and to acknowledge Prof. Alasdair McGowan and Dr. Andrew Lovering at the Bristol Antimicrobial Reference Laboratory for analysis of blood and microdialysis samples. We would like to acknowledge the National Institute for Health Research Health Protection Research Unit (NIHR HPRU) in Healthcare Associated Infections and Antimicrobial Resistance at Imperial College London in partnership with Public Health England. This research was cofunded by the NIHR Imperial Biomedical Research Centre, Institut Mérieux and Innovate UK (Project Number 5397) and was supported by the NIHR Imperial Clinical Research Facility. AH is an NIHR Senior Research Investigator and TR is funded by the National Institute for Health Research Invention for Innovation Grant (i4i), Enhanced, Personalised and Integrated Care for Infection Management at Point of Care (EPIC IMPOC), II-LA-0214-20008. The views expressed are those of the authors and not necessarily those of the NHS, the NIHR or the Department of Health and Social Care.

■ REFERENCES

(1) O'Neill, J. *Antimicrobial Resistance: Tackling a Crisis for the Health and Wealth of Nations*; 2014. DOI: 10.1038/510015a.

(2) Holmes, A. H.; Moore, L. S. P.; Sundsfjord, A.; Steinbakk, M.; Regmi, S.; Karkey, A.; Guerin, P. J.; Piddock, L. J. V. Understanding the Mechanisms and Drivers of Antimicrobial Resistance. *Lancet* **2016**, *387* (10014), 176–187.

(3) Mouton, J. W.; Ambrose, P. G.; Canton, R.; Drusano, G. L.; Harbarth, S.; Macgowan, A.; Theuretzbacher, U.; Turnidge, J. Conserving Antibiotics for the Future : New Ways to Use Old and

DOI: 10.1021/acssensors.9b00288
ACS Sens. 2019, 4, 1072–1080

New Drugs from a Pharmacokinetic and Pharmacodynamic Perspective. *Drug Resist. Updates* **2011**, *14* (2), 107−117.
(4) Roberts, J. A.; Ulldemolins, M.; Roberts, M. S.; McWhinney, B.; Ungerer, J.; Paterson, D. L.; Lipman, J. Therapeutic Drug Monitoring of β-Lactams in Critically Ill Patients: Proof of Concept. *Int. J. Antimicrob. Agents* **2010**, *36* (4), 332−339.
(5) Roberts, J. A.; Abdul-Aziz, M. H.; Lipman, J.; Mouton, J. W.; Vinks, A. A.; Felton, T. W.; Hope, W. W.; Farkas, A.; Neely, M. N.; Schentag, J. J.; et al. Individualised Antibiotic Dosing for Patients Who Are Critically Ill: Challenges and Potential Solutions. *Lancet Infect. Dis.* **2014**, *14* (6), 498−509.
(6) Han, S.; Li, B.; Song, Z.; Pan, S.; Zhang, Z.; Yao, H.; Zhu, S.; Xu, G. A Kanamycin Sensor Based on an Electrosynthesized Molecularly Imprinted Poly-: O -Phenylenediamine Film on a Single-Walled Carbon Nanohorn Modified Glassy Carbon Electrode. *Analyst* **2017**, *142* (1), 218−223.
(7) Rowe, A. A.; Miller, E. A.; Plaxco, K. W. Reagentless Measurement of Aminoglycoside Antibiotics in Blood Serum via an Electrochemical, Ribonucleic Acid Aptamer-Based Biosensor. *Anal. Chem.* **2010**, *82* (17), 7090−7095.
(8) Ferguson, B. S.; Hoggarth, D. A.; Maliniak, D.; Ploense, K.; White, R. J.; Woodward, N.; Hsieh, K.; Bonham, A. J.; Eisenstein, M.; Kippin, T. E. Real-Time, Aptamer-Based Tracking of Circulating Therapeutic Agents in Living Animals. *Sci. Transl. Med.* **2013**, *5* (213), 213ra165.
(9) Daprà, J.; Lauridsen, L. H.; Nielsen, A. T.; Rozlosnik, N. Comparative Study on Aptamers as Recognition Elements for Antibiotics in a Label-Free All-Polymer Biosensor. *Biosens. Bioelectron.* **2013**, *43* (1), 315−320.
(10) Huet, A. C.; Delahaut, P.; Fodey, T.; Haughey, S. A.; Elliott, C.; Weigel, S. Advances in Biosensor-Based Analysis for Antimicrobial Residues in Foods. *TrAC, Trends Anal. Chem.* **2010**, *29* (11), 1281−1294.
(11) Rawson, T. M.; Sharma, S.; Georgiou, P.; Holmes, A.; Cass, A.; O'Hare, D. Towards a Minimally Invasive Device for Beta-Lactam Monitoring in Humans. *Electrochem. Commun.* **2017**, *82* (July), 1−5.
(12) Gustavsson, E.; Sternesjo, A. Biosensor Analysis of β-Lactams in Milk: Comparison with Microbiological Immunological and Receptor-Based Screening Methods. *J. AOAC Int.* **2004**, *87* (3), 614−620.
(13) Müller, C.; Hitzmann, B.; Schubert, F.; Scheper, T. Optical Chemo- and Biosensors for Use in Clinical Applications. *Sens. Actuators, B* **1997**, *40* (1), 71−77.
(14) Healey, B. G.; Li, L.; Walt, D. R. Multianalyte Biosensors on Optical Imaging Bundles. *Biosens. Bioelectron.* **1997**, *12* (6), 521−529.
(15) Conzuelo, F.; Gamella, M.; Campuzano, S.; Martínez-Ruiz, P.; Esteban-Torres, M.; De Las Rivas, B.; Reviejo, A. J.; Muñoz, R.; Pingarrón, J. M. Integrated Amperometric Affinity Biosensors Using Co2+- Tetradentate Nitrilotriacetic Acid Modified Disposable Carbon Electrodes: Application to the Determination of β-Lactam Antibiotics. *Anal. Chem.* **2013**, *85* (6), 3246−3254.
(16) Gustavsson, E.; Bjurling, P.; Degelaen, J.; Sternesjö, Å. Analysis of β-Lactam Antibiotics Using a Microbial Receptor Protein-Based Biosensor Assay. *Food Agric. Immunol.* **2002**, *14* (2), 121−131.
(17) Babington, R.; Matas, S.; Marco, M.-P.; Galve, R. Current Bioanalytical Methods for Detection of Penicillins. *Anal. Bioanal. Chem.* **2012**, *403* (6), 1549−1566.
(18) Schoning, M. J.; Kurowski, A.; Thust, M.; Kordos, P.; Schultze, J. W.; Lüth, H. Capacitive Microsensors for Biochemical Sensing Based on Porous Silicon Technology. *Sens. Actuators, B* **2000**, *64* (1−3), 59−64.
(19) Sternesjo, A.; Gustavsson, E. Biosensor Analysis of Beta-Lactams in Milk Using the Carboxypeptidase Activity of a Bacterial Penicillin Binding Protein. *J. AOAC Int.* **2006**, *89* (3), 832−837.
(20) Stred'Anský, M.; Pizzariello, A.; Stred'Anská, S.; Miertuš, S. Amperometric PH-Sensing Biosensors for Urea, Penicillin, and Oxalacetate. *Anal. Chim. Acta* **2000**, *415* (1−2), 151−157.
(21) Thust, M.; Schöning, M. J.; Vetter, J.; Kordos, P.; Lüth, H. A Long-Term Stable Penicillin-Sensitive Potentiometric Biosensor with Enzyme Immobilized by Heterobifunctional Cross-Linking. *Anal. Chim. Acta* **1996**, *323* (1−3), 115−121.
(22) Nishizawa, M.; Matsue, T.; Uchida, I. Fabrication of a PH-Sensitive Micro-Array Electrode and Applicability to Biosensors. *Sens. Actuators B* **1993**, *B13* (1−3), 53−56.
(23) Brand, U.; Reinhardt, B.; Ruether, F.; Scheper, T.; Schuegerl, K. Bio-Field-Effect Transistors as Detectors in Flow-Injection Analysis. *Anal. Chim. Acta* **1990**, *238* (1), 201−210.
(24) Gustavsson, E.; Bjurling, P.; Sternesjoe, A. Biosensor Analysis of Penicillin G in Milk Based on the Inhibition of Carboxypeptidase Activity. *Anal. Chim. Acta* **2002**, *468* (1), 153−159.
(25) Leszczyńska, E.; Głąb, S.; Sokół, A.; Dzięgielewski, K.; Rokicka, R.; Koncki, R. Potentiometric Biosensor for Control of Biotechnological Production of Penicillin G. *Anal. Chim. Acta* **1998**, *368* (3), 205−210.
(26) Seki, A.; Ikeda, S.-I.; Kubo, I.; Karube, I. Biosensors Based on Light-Addressable Potentiometric Sensors for Urea. *Anal. Chim. Acta* **1998**, *373* (1), 9−13.
(27) Simonis, A.; Ruge, C.; Müller-Veggian, M.; Lüth, H.; Schöning, M. J. A Long-Term Stable Macroporous-Type EIS Structure for Electrochemical Sensor Applications. *Sens. Actuators, B* **2003**, *91* (1−3), 21−25.
(28) Sinnollareddy, M. G.; Roberts, M. S.; Lipman, J.; Lassig-Smith, M.; Starr, T.; Robertson, T.; Peake, S. L.; Roberts, J. A. In Vivo Microdialysis to Determine Subcutaneous Interstitial Fluid Penetration and Pharmacokinetics of Fluconazole in Intensive Care Unit Patients with Sepsis. *Antimicrob. Agents Chemother.* **2016**, *60* (2), 827−832.
(29) Ranamukhaarachchi, S. A.; Padeste, C.; Dübner, M.; Häfeli, U. O.; Stoeber, B.; Cadarso, V. J. Integrated Hollow Microneedle-Optofluidic Biosensor for Therapeutic Drug Monitoring in Sub-Nanoliter Volumes. *Sci. Rep.* **2016**, *6* (July), 1−10.
(30) Sharma, S.; El-Laboudi, A.; Reddy, M.; Jugnee, N.; Sivasubramaniyam, S.; El Sharkawy, M.; Georgiou, P.; Johnston, D.; Oliver, N.; Cass, A. E. G. A Pilot Study in Humans of Microneedle Sensor Arrays for Continuous Glucose Monitoring. *Anal. Methods* **2018**, *10* (18), 2088−2095.
(31) Sharma, S.; Saeed, A.; Johnson, C.; Gadegaard, N.; Cass, A. E. Rapid, Low Cost Prototyping of Transdermal Devices for Personal Healthcare Monitoring. *Sens. Bio-Sensing Res.* **2017**, *13*, 104−108.
(32) Mishra, R. K.; Vinu Mohan, A. M.; Soto, F.; Chrostowski, R.; Wang, J. Microneedle Biosensor for Minimally-Invasive Transdermal Detection of Nerve Agents. *Analyst* **2017**, *142*, 918−924.
(33) Miller, P. R.; Narayan, R. J.; Polsky, R. Microneedle-Based Sensors for Medical Diagnosis. *J. Mater. Chem. B* **2016**, *4* (8), 1379−1383.
(34) El-Laboudi, A.; Oliver, N. S.; Cass, A.; Johnston, D. Use of Microneedle Array Devices for Continuous Glucose Monitoring: A Review. *Diabetes Technol. Ther.* **2013**, *15* (1), 101−115.
(35) Cha, K. J.; Kim, T.; Park, S. J.; Kim, D. S. Simple and Cost-Effective Fabrication of Solid Biodegradable Polymer Microneedle Arrays with Adjustable Aspect Ratio for Transdermal Drug Delivery Using Acupuncture Microneedles. *J. Micromech. Microeng.* **2014**, *24* (11), 115015.
(36) Lee, H.; Song, C.; Hong, Y. S.; Kim, M. S.; Cho, H. R.; Kang, T.; Shin, K.; Choi, S. H.; Hyeon, T.; Kim, D. H. Wearable/Disposable Sweat-Based Glucose Monitoring Device with Multistage Transdermal Drug Delivery Module. *Sci. Adv.* **2017**, *3* (3), e1601314.
(37) Sullivan, S. P.; Murthy, N.; Prausnitz, M. R. Minimally Invasive Protein Delivery with Rapidly Dissolving Polymer Microneedles. *Adv. Mater.* **2008**, *20* (5), 933−938.
(38) Kim, Y. C.; Park, J. H.; Prausnitz, M. R. Microneedles for Drug and Vaccine Delivery. *Adv. Drug Delivery Rev.* **2012**, *64* (14), 1547−1568.
(39) Cullen, L. F.; Rusling, J. F.; Schleifer, A.; Papariello, G. J. Improved Penicillin Selective Enzyme Electrode. *Anal. Chem.* **1974**, *46* (13), 1955−1961.

DOI: 10.1021/acssensors.9b00288
ACS Sens. 2019, 4, 1072−1080

(40) Ng, S. R.; O'Hare, D. An Iridium Oxide Microelectrode for Monitoring Acute Local PH Changes of Endothelial Cells. *Analyst* **2015**, *140* (12), 4224−4231.
(41) Yamanaka, K. Anodically Electrodeposited Iridium Oxide Films (AEIROF) from Alkaline Solutions for Electrochromic Display Devices. *Jpn. J. Appl. Phys.* **1989**, *28* (4 R), 632−637.
(42) Bond, J. M.; Lightbown, J. W.; Barber, M.; Waterworth, P. M. A Comparison of Four Phenoxypenicillins. *Br. Med. J.* **1963**, *2*, 956−961.
(43) Tan, J. S.; Trott, A.; Phair, J. P.; Watanakunakorn, C. A Method for Measurement of Antibiotics in Human Interstitial Fluid. *J. Infect. Dis.* **1972**, *126* (5), 492−497.
(44) Vasylieva, N.; Barnych, B.; Meiller, A.; Maucler, C.; Pollegioni, L.; Lin, J.-S.; Barbier, D.; Marinesco, S. Covalent Enzyme Immobilization by Poly(Ethylene Glycol) Diglycidyl Ether (PEGDE) for Microelectrode Biosensor Preparation. *Biosens. Bioelectron.* **2011**, *26* (10), 3993−4000.

DOI: 10.1021/acssensors.9b00288
ACS Sens. 2019, 4, 1072−1080